

Modeling the 3D Spatiotemporal Organization of Chromatin Replication

G. Forte¹, S. Buonomo², P. R. Cook³, N. Gilbert⁴, D. Marenduzzo¹ and E. Orlandini⁵

¹*SUPA, School of Physics and Astronomy, University of Edinburgh, Peter Guthrie Tait Road, Edinburgh EH9 3FD, United Kingdom*

²*Institute of Cell Biology, School of Biological Sciences, University of Edinburgh, Edinburgh EH9 3FF, United Kingdom*

³*Sir William Dunn School of Pathology, University of Oxford, South Parks Road, Oxford OX1 3RE, United Kingdom*

⁴*MRC Human Genetics Unit, MRC Institute of Genetics and Cancer, University of Edinburgh, Western General Hospital, Edinburgh EH4 2XU, United Kingdom*

⁵*Dipartimento di Fisica e Astronomia and Sezione INFN, Università di Padova, Via Marzolo 8, Padova 35131, Italy*



(Received 22 March 2024; accepted 9 September 2024; published 26 September 2024)

We propose a polymer model to investigate *in silico* the dynamics of chromatin replication in three dimensions (PolyRep). Our results indicate that replication complexes, the replisomes, may self-assemble during the process and replicate chromatin by extruding it (immobile replisome) or by moving along the template filament (tracking replisome), reconciling previous discordant experimental evidence in favour of either scenario. Importantly, the emergence of one of the two morphologies depends in a major way on the replication origin distribution as well as on the presence of nonspecific interactions between unreplicated chromatin and firing factors—polymerases and other components of the replisome. Nonspecific interactions also appear instrumental to creating clusters of factors and replication forks, structures akin to the replication foci observed in mammalian cells *in vivo*. PolyRep simulations predict different mechanisms for foci evolution, including unanticipated loop-mediated fusion dynamics. We suggest that cluster formation, which our model suggests to be a generic feature of chromatin replication, provides a hitherto underappreciated but robust pathway to avoid stalled or faulty forks, which would otherwise diminish the efficiency of the replication process.

DOI: [10.1103/PRXLife.2.033014](https://doi.org/10.1103/PRXLife.2.033014)

I. INTRODUCTION

Replication of eukaryotic DNA and chromatin is a crucial process in a cell's lifecycle. While normally depicted in one dimension (1D), it is inherently a three-dimensional (3D) process, in which spatiotemporal organization is important [1]. Two main models describe such organization [2,3]. In the *tracking* model (Fig. 1, left), two replisomes loaded on one origin move away from each other as they replicate. In the *immobile replisome* model (Fig. 1, right), the two are instead in constant contact, as template DNA is pulled in from each side and two double-stranded loops are extruded. There is evidence for and against both models. On the one hand, fork progression *in vitro* is unaffected by omitting from the reaction the Ctf4 molecules that hold the two helicases together in the pre-replication complex [4], and single-molecule imaging of extracts from *Xenopus* eggs reveals individual replisomes tracking independently along templates [5]. On the other hand, structures of replication complexes assembled *in vitro* are consistent with a central and immobile dimer that extrudes daughter duplexes [6], and more evidence for the immobile replisome model is reviewed in [7]. Experiments on bacteria also suggest that both models may apply in a single cell, as replisomes are at times moving together, and at others tracking independently [8].

Besides being an integral part of the immobile replisome model, clusters (of polymerases and replisome elements) are also observed at a higher level in chromatin organization [9]. Thus, many human replisome pairs have been found to form clusters, called replication *foci* or *factories*. Such clusters are usually small at the beginning of the S phase, before enlarging and changing nuclear position [10,11]. Notably, mechanisms leading to the change in foci size remain unclear. For instance, early experiments suggested that mammalian foci are fixed in 3D space and the clustering observed during S-phase is due to continuous disassembly and reassembly of whole replisomes [12], while more recent work shows mobile yeast foci continuously fusing and segregating [13].

The replication fork—the DNA sites where a helicase and polymerases are working together to replicate the genomic material—moves at a speed that depends on the organism, with an average of 1.6–3 kb/min in yeast [14]. Forks are normally thought to be asymmetric, such that the leading strand is synthesized almost continuously, whereas the lagging strand is replicated by stitching together short Okazaki fragments, and the polymerase on the lagging strand disengages often. Additionally, obstacles such as RNA polymerases or DNA damage can slow or stall forks—on either the leading or lagging strand—and this can induce replication stress and the development of common fragile sites [15,16]. Recent single-molecule photobleaching experiments show that most components in bacterial and yeast replisomes (even leading-strand polymerases) exchange rapidly and continuously with the soluble pool [17], and this could facilitate the progress of a fork halted by a blockage [18]. Consequently, one may imagine

Published by the American Physical Society under the terms of the [Creative Commons Attribution 4.0 International](https://creativecommons.org/licenses/by/4.0/) license. Further distribution of this work must maintain attribution to the author(s) and the published article's title, journal citation, and DOI.

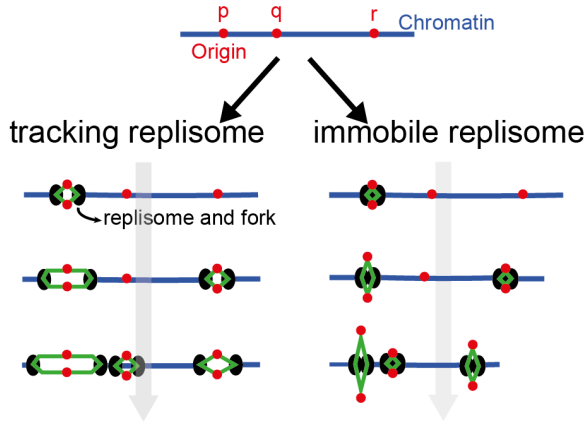


FIG. 1. Replication by tracking or immobile replisomes. In the tracking model (left), two replisomes bind to origin p , create a replication bubble, and move apart as they generate two new double helices (green segments); the process is repeated at q and r . If immobile (right), two replisomes bind to origin p and remain together as each pulls in template DNA and extrudes two new daughter helices; as before, the process repeats at q and r . Note that each replisome in a pair is immobile relative to its partner, but pairs still move relative to other pairs. In both scenarios, the transparent gray arrow indicates time evolution.

that the system has to strike a compromise between the tight binding required to keep replisomes on the DNA, while allowing a sufficiently dynamic exchange to avoid stalling.

While many models describing replication dynamics and origin firing have been developed (see, e.g., [19–25]), most are inherently 1D and very few include the critical role played by 3D effects and polymer physics, which are also relevant for chromatin organization [26–28]. Modeling spatial patterns in eukaryotic replication is complicated because a newly replicated polymer with its steric hindrance has to be dynamically created; additionally, one has to account for the binding-unbinding dynamics of firing factors—identified here as polymerases and other replisome elements—which is not well characterized experimentally. Nevertheless, this type of modeling has the potential to generate new hypotheses to be tested experimentally, which go beyond the prediction of firing efficiency and replication profiles along the 1D genome.

To address this gap, here we develop PolyRep, a 3D polymer model to study the dynamics of chromatin replication and, in particular, of clusters of firing factors and forks (i.e., replication factories/foci). This model is minimal in the sense that as few parameters as possible have been retained to describe this complex system, yet the model can both reproduce some key properties of eukaryotic replication and also identify what are the crucial ingredients for its spatial organization in 3D. First, we show that in simulations both the immobile and the tracking replisome models can be observed. The balance between the two depends on the ratio between nonspecific interactions between firing factors and chromatin, and specific interactions between factors and origins. The presence of nonspecific interactions is pivotal in simulations to observe the immobile replisome scenario, and in general for the formation of clusters of factors and origins. These results lead us to speculate that the emerging clusters may have a functional role, as

they fuel the restarting of replication when polymerases are temporarily lost, as could happen in reality after the replication of an Okazaki fragment. This is important biologically, as stalled forks would hinder the efficiency of the replication process. Second, simulations suggest different scenarios for the spatiotemporal evolution of the replication foci/factories. Thus, clusters in our simulations may grow by collisions, or by a new and unexpected formation of long-range chromatin loops, which could be tested in future experiments.

II. RESULTS

A. PolyRep—A 3D polymer model for chromatin replication

In this study we develop PolyRep, a coarse-grained polymer model to study replication of chromatin. Critically, our new PolyRep model is based on as few assumptions as possible, such that it could be applied throughout eukaryotes despite considerable variations in origin size, spacing, and firing frequency [29–32]. Chromatin is depicted as a semiflexible polymer composed of a sequence of beads connected by springs (Fig. 2). Each bead is assumed to have a diameter $\sigma = 15$ nm and contains 1 kbp of DNA [33]. An additional potential among triplets of consecutive beads provides a persistence length $l_p \sim 60$ nm, approximately that of chromatin [34,35] (see Material and Methods for details). A chromatin fiber initially contains two types of sites: unreplicated chromatin sites (blue beads in Fig. 2) and replication origins (red beads in Fig. 2). All proteins required for replication are represented by brown spheres, which we call “firing factors” (FFs), and include all components necessary to complete a whole replication cycle (i.e., activating kinases, MCM proteins, helicases, polymerases replicating leading and lagging strands, topoisomerases, PCNA, and termination proteins). Importantly, the concentration of FFs in our simulations is limiting, meaning that only a few origins in a multiorigin chromatin fiber can be active at any time, as observed *in vivo* [36].

FFs diffuse throughout space while being excluded from the volume occupied by all other beads (Fig. 2). Their multivalent binding to different types of chromatin beads is modeled by a truncated and shifted Lennard-Jones potential

$$V_{\text{LJ/cut}}(r_{i,j}) = [V_{\text{LJ}}(r_{i,j}) - V_{\text{LJ}}(r_c)]\Theta(r_c - r_{i,j}), \quad (1)$$

where $r_{i,j}$ is the distance between the i th and j th beads, $r_c = 1.8\sigma$ is a cutoff distance, and

$$V_{\text{LJ}}(r) = 4\varepsilon \left[\left(\frac{\sigma}{r_{i,j}} \right)^{12} - \left(\frac{\sigma}{r_{i,j}} \right)^6 \right], \quad (2)$$

with ε being the interaction energy. As FFs can mimic protein complexes, rather than single proteins, multivalency is likely to be a generic feature, as it can arise from single valence interactions from different components of the complex.

FFs are assumed to be nonspecifically (weakly) attracted to unreplicated (blue) chromatin beads [$\varepsilon = \varepsilon_{\text{ns}} = 4k_B T$ in Eq. (2)] and moderately to (red) origins [$\varepsilon = \varepsilon_{\text{origin}} = 6k_B T$ in Eq. (2)]. The importance of a weak interaction between FFs and unreplicated chromatin beads is explained below and represents a key feature of our model. The existence of such nonspecific interactions is a natural assumption given generic properties of chromatin-binding proteins arising from

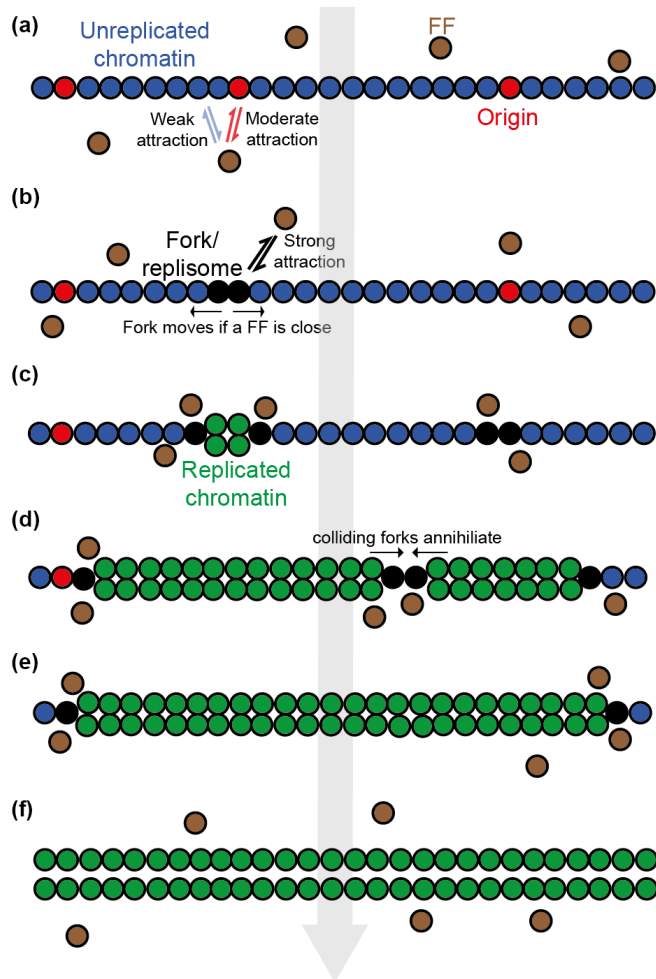


FIG. 2. A 3D polymer model for chromatin replication. Chromatin is represented as a polymer composed of several beads, each one corresponding to 1 kbp. The light gray arrow, from top to bottom, indicates the time evolution of the system. (a) Initially, chromatin contains unreplicated sites (blue beads) and replication origins (red beads). Firing factors (FFs, brown spheres) bind weakly (nonspecifically) to unreplicated chromatin sites and strongly to replication origins. (b) When an FF binds to an origin, the origin *fires* with probability P_{fire} ; this involves converting the origin plus one of its randomly chosen neighbors into two forks or replisomes (black beads) which attract FFs very strongly. (c) The two forks independently move in opposite directions whenever a FF is close by. This bidirectional replication results in the formation of two chromatin fibers (green beads) which only interact with FFs sterically. (d), (e) The collision of two forks results in their annihilation, and the replicated fibers generated by each fork join together. (f) Replication ends when the whole string is “replicated” into two green strings.

chromatin immunoprecipitation (or ChIP-seq) experiments, where the background signal is usually associated with weak (nonspecific) binding, while peaks are associated with high-affinity (sequence-specific) interactions. Additionally, weak sequence-independent attractions, primarily due to electrostatic interactions, have been observed for several bacterial DNA-binding proteins [37], and for some eukaryotic transcription factors, where they contribute to 1D facilitated diffusion to locate their target on the genome [38].

Replication is then modeled as follows. Once a FF binds to an origin [Fig. 2(a)], the latter fires with probability P_{fire} to create a pair of replisomes or forks [two black beads derived from the red bead plus a randomly chosen blue neighbor; Fig. 2(b)]. Each fork binds FFs strongly [$\epsilon = \epsilon_{\text{fork}} = 10k_B T$ in Eq. (2)] and moves independently and in the opposite direction to its partner, provided that an FF is nearby (within $r_c = 1.8\sigma$). The fork movement along the template chromatin strand results in the replication of the template strand itself and the formation of a new strand [green beads; Fig. 2(c)]. Both strands are identical with respect to their biophysical properties and only interact through steric repulsion with FFs. During the simulation multiple origins can fire, and when two forks traveling in opposite directions collide [Fig. 2(d)], they annihilate each other to leave appropriately connected replicated chains [Figs. 2(d) and 2(e)]. Through successive origin firing events and fork movements, the original (blue/red) chain is replaced by two replicated (green) chains that separate at the end of replication [Fig. 2(f)]. The final two replicated fibers cannot be re-replicated (in accordance with what is seen *in vivo* [39]) as they contain no “licensed” origins, and as we assume FFs have no affinity for green replicated beads due to the temporary disruption of the chromatin structure and loss of epigenetic information occurring during replication [40,41].

The entire system is subject to Brownian dynamics, which is integrated through the software LAMMPS [42].

B. Replicating a chromatin fiber with one origin

We start by analyzing the replication of a chromatin fibre formed by 1000 beads (equivalent to 1 Mbp), with a single origin in the middle, and surrounded by 20 firing factors. The origin fires with probability $P_{\text{fire}} = 0.01$. Unless specified otherwise, this firing frequency will be used throughout, as it is close to the median of 0.037 obtained for human initiation zones [30], and because it gives sufficiently slow dynamics to be biophysically realistic, while remaining computationally tractable.

In our PolyRep simulations, FFs often form agglomerates spontaneously. Notably, this phenomenon occurs in the absence of any attractive interaction between FFs, but it is due to a positive feedback mechanism known as bridging-induced phase separation (BIPS) that depends on multivalent bindings of FFs on chromatin. This feedback works as follows [43,44]: the initial nonspecific binding of an FF to a chromatin segment results in an increase in the local chromatin density that, in turn, attracts more FFs giving rise to FF agglomerates [see Fig. S1(a) in the Supplemental Material (SM) [45]]. Such agglomerates can be partitioned as follows: those that are spatially close to more than one fork (we shall call them *clusters*), and all others (we shall call them *aggregates*); see Fig. S1(b). In this context, clusters are analogous to replication factories, or foci. Note that, within the immobile replisome scenario, such clusters can arise also if a single origin is present as two forks colocalize.

In a typical simulation (Movie S1 in the SM [45]), the system is initialized with a relaxed chain and diffusing (but nonbinding) FFs [Fig. 3(a)]. As soon as the attraction between FFs and chromatin sets in, BIPS drives the spontaneous formation of FF aggregates ahead of replication [Fig. 3(b)].

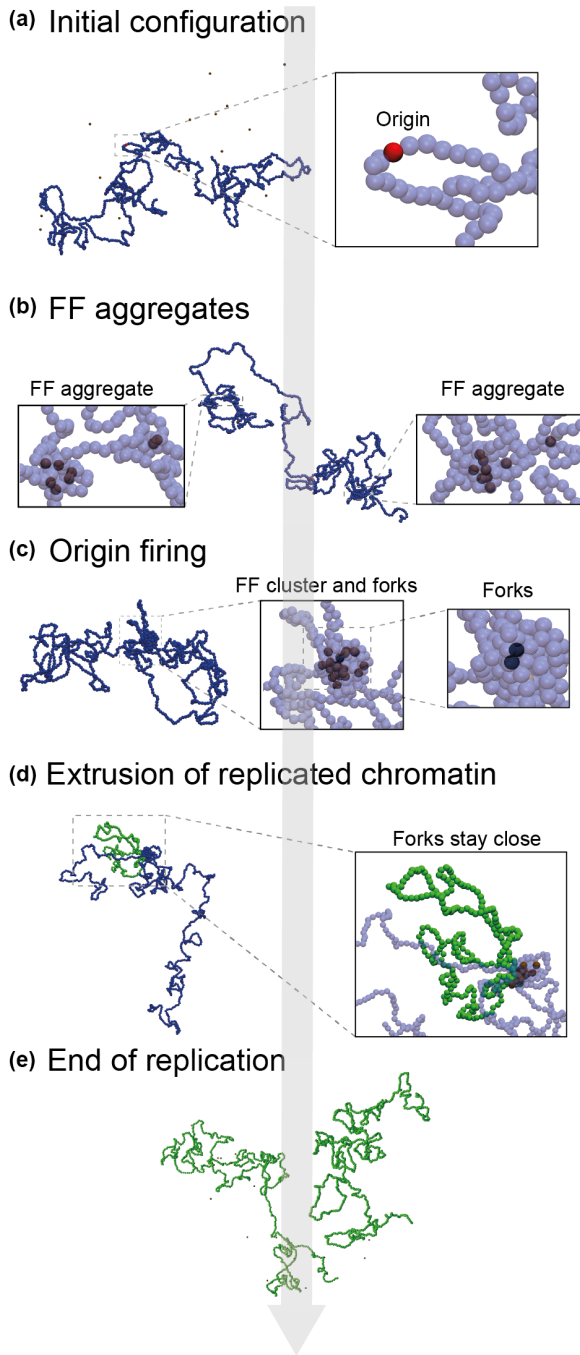


FIG. 3. Frames from a simulation about replication of a chromatin fiber with a single origin. (a) Initial configuration containing the relaxed chromatin fiber and diffusing FFs. The chromatin polymer is composed of 1000 beads (1 Mbp) and the origin is placed in the middle. Blue beads in the inset are represented as transparent to highlight the origin (the same representation will be used in the following panels). (b) After switching on the attraction between FFs and chromatin, FF aggregates form. (c) When an FF aggregate gets close to the origin, the latter fires with probability $P_{\text{fire}} = 0.01$, resulting in the formation of two forks—the FF aggregate is now an FF cluster or replication factory/foci. (d) Replicated chromatin is extruded by the two forks that stay close in 3D throughout the whole replication process. (e) The simulation ends when the whole initial chromatin fiber has been replicated, leaving two separate fibers.

Eventually, in the setup of Fig. 3, all FFs localize close to the replication origin (where the affinity is larger). When the origin fires, a pair of forks/replisomes are formed. This is surrounded by an FF cluster, which can be identified as a replication factory [Fig. 3(c)]. Strikingly, the resulting forks remain close in 3D space throughout replication [Fig. 3(d)] despite the absence of any direct force between them. At the end of the simulation, the two replicated fibers finally diffuse independently from each other and separate [Fig. 3(e)].

This simple model captures some key elements of replication *in vivo*—mainly, the extrusion of two daughter loops by a replisome pair, and the maintenance of contact between the two replisomes in a pair. Importantly, the crucial element to maintaining the two replisomes together is the presence of a weak nonspecific attraction and the consequent formation of the FF cluster, as we will quantitatively demonstrate next.

C. Nonspecific interactions are required to keep replisomes together

We now examine the role of the weak nonspecific attraction, between FFs and unreplicated chromatin sites that are not origins (blue beads in Fig. 2), in the formation of a replisome pair. We ask whether without nonspecific attractions the two forks can remain close in 3D throughout replication. To address this question, we perform simulations where we keep the parameters of the model as previously ($\epsilon_{\text{origin}} = 6k_B T$, $\epsilon_{\text{fork}} = 10k_B T$), but now we remove the nonspecific attraction between unreplicated (blue) chromatin beads and FFs. The firing probability has been increased here to $P_{\text{fire}} = 1$ to speed up simulations; the results are not qualitatively affected by this different value. Importantly, without nonspecific interactions, FF agglomerates or clusters are not observed, and—once the origin fires—the two replisomes track separately (Movie S2).

By increasing the value of ϵ_{fork} sufficiently, one would expect that a single FF will be able to bind the two forks so strongly as to keep them together during the whole replication process, without requiring the presence of an FF cluster. While this is true, the value required for this to occur corresponds to $\epsilon_{\text{fork, min}} > 50k_B T$, which is unrealistically large, as we now show. To compare with realistic affinities between forks and FFs, we use statistical mechanics to relate the Lennard-Jones potential in Eq. (1) (and hence ϵ_{fork}) to the dissociation constant K_D , which is used more commonly in biochemistry to determine the strength of a ligand-protein interaction, and which equals the concentration of ligands for which half proteins are bound [46].

The equation relating ϵ_{fork} to K_D is (see the SM for details)

$$\frac{1}{K_D} = 4\pi \int_0^{r_c} x^2 \exp \left[-4\beta\epsilon_{\text{fork}} \left(\frac{1}{x^{12}} - \frac{1}{x^6} \right) \right] dx, \quad (3)$$

where r_c is the Lennard-Jones cutoff distance $r_c = 1.8\sigma$. The K_D required to keep two forks together (corresponding to $\epsilon_{\text{fork, min}} > 50k_B T$) is then sub-picomolar ($K_{D, \text{min}} \ll 1$ pM), far smaller than the smallest nanomolar dissociation constants found *in vivo* [1]. We conclude that, in the absence of nonspecific interactions between FFs and chromatin, replisome pairing requires unrealistically small dissociation constants, hence it would not be observed, and replisomes would track

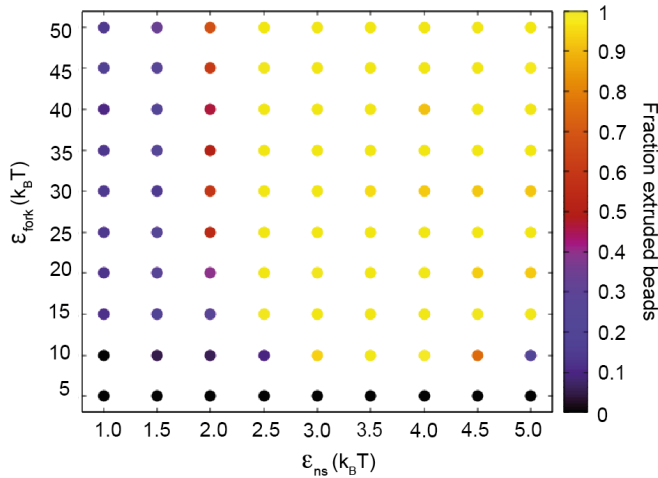


FIG. 4. Phase diagram for the fraction of extruded beads in a chromatin fiber composed of 1000 beads with a single origin in the middle. The phase diagram shows the fraction of extruded beads (color scale on the right) depending on ε_{ns} (x -axis) and $\varepsilon_{\text{fork}}$ (y -axis). The fraction of extruded beads is defined as the fraction of beads that have been replicated in the presence of an immobile replisome scenario and, hence, have been extruded by a pair of forks (see the SM for more details). The attraction between FFs and the origin, $\varepsilon_{\text{origin}}$, is kept constant and equal to $6k_B T$, while the number of FFs is set equal to 20 (considering a different number of FFs does not significantly change the results; see Fig. S2). For each couple of parameters (ε_{ns} , $\varepsilon_{\text{fork}}$), the fraction of extruded beads is computed by averaging over 10 independent simulations. Black dots correspond to cases when the replication process is so slow that only very few beads (less than 2%) have been replicated during the simulation time. This results in unrealistic total replication times and in the impossibility of computing a statistically significant fraction of extruded chromatin.

independently. A phase diagram showing more quantitatively the balance between extrusion and tracking as a function of ε_{ns} (x -axis) and $\varepsilon_{\text{fork}}$ (y -axis) is shown in Fig. 4. It can be seen that at low ε_{ns} tracking dominates, whereas extrusion takes over when the nonspecific attraction between FFs and unreplicated chromatin sites increases, such that a cluster can be formed to immobilize the two replisomes in 3D (a more quantitative analysis of the effects of nonspecific interactions on the chromatin crowdedness in proximity to FFs and forks is shown in Fig. S3). Interestingly, for larger values of ε_{ns} , the fraction of extruded beads decreases [see, for instance, the points $(\varepsilon_{\text{ns}}, \varepsilon_{\text{fork}}) = (4.5k_B T, 10k_B T)$ and $(\varepsilon_{\text{ns}}, \varepsilon_{\text{fork}}) = (5k_B T, 10k_B T)$] as the value of ε_{ns} becomes comparable to that of $\varepsilon_{\text{fork}}$. This leads to increased competition for FFs between forks and unreplicated chromatin and suggests that the efficiency and relevance of the extrusion mechanism depend on the ratio between $\varepsilon_{\text{fork}}$ and ε_{ns} .

The phase diagram in Fig. 4 and the calculation in Eq. (3) demonstrate that nonspecific interactions are crucial to observe replisome pairing concomitant with FF clustering. As previously mentioned, although the weak affinity of replisome elements for nonorigin sites has yet to be experimentally proven, its existence is plausible based on existing experimental evidence (for instance from chromatin immunoprecipitation).

D. Replicating a chromatin fiber with multiple origins

As chromosomes in eukaryotes contain multiple replication origins, we next consider a chain composed of 1000 beads (representing 1 Mbp) with 10 equally spaced origins [Fig. 5(a) (i)], each of them firing with probability $P_{\text{fire}} = 0.01$. As in the single origin case, the system contains 20 firing factors with weak attraction to unreplicated chromatin and strong attraction to replication forks. We note that this setup with multiple origins yields budding yeast replication profiles in agreement with the experimental ones published in Ref. [47] (Fig. S4). In this setup, multiple replisome pairs can be active at the same time (see Movie S3), which speeds up the replication process. The temporal evolution of replication can conveniently be depicted using a kymograph, where, for each time point (x -axis), differently colored chromatin beads (whose index is reported in the y -axis) are represented by appropriately colored pixels [Fig. 5(a) (ii)]. Origin firing and fork merging are marked by green peaks and valleys, respectively. In the plot, the formation of multiple fork pairs (like those created by origins close to beads 250 and 750) can be observed, as well as the passive replication of origins that do not fire during the simulation (like the origin close to the bead 1000). Such stochastic and infrequent firing is the norm in mammalian cells [30].

E. Clusters of forks and firing factors form and grow spontaneously

Previous microscopy experiments revealed the formation and growth of clusters (or replication factories) by tracking both elements of the replication machine [48] and forks [48,49]. To address such dynamics by PolyRep simulations, the evolution of clusters of FFs and forks, which are the equivalent to replication factories/foci *in silico*, was analyzed during the replication of a chromatin fiber containing 10 equally spaced origins. To investigate the number and size of clusters, we use the algorithm provided in [50], and we say that two particles (either two forks or two FFs) belong to the same cluster if their 3D distance is smaller than $r_{\text{thre}} = 4\sigma$ for forks and $r_{\text{thre}} = 2\sigma$ for FFs (small variations in r_{thre} do not change the results). The cluster size is then defined as the number of particles composing the cluster.

Clustering dynamics predicted by PolyRep simulations with multiple origins can be summarized as follows. First, FF clusters form as forks originating from different origins come together (see Movie S3). The underlying mechanism is again driven by BIPS. Second, Fig. 5(b) shows the total number of forks and FFs in clusters, the number and size of forks and FF clusters, and the fraction of replicated chromatin, averaged over 20 independent simulations. The curves for fork cluster size and number show a nonmonotonic behavior in time [Fig. 5(b) (i)]. In more detail, the initial firing of the replication origins leads to the formation of several pairs of forks and the consequent increase in the number of clusters and the cluster size. For $t \geq 0.8 \times 10^6 \tau_B$, when about 45% of chromatin has been replicated, the number of clusters of forks starts decreasing, while the average cluster size and the number of forks still display peaks, due to the firing of new origins.

A more direct comparison with experimental findings based on microscopy imaging [2] of replication factory

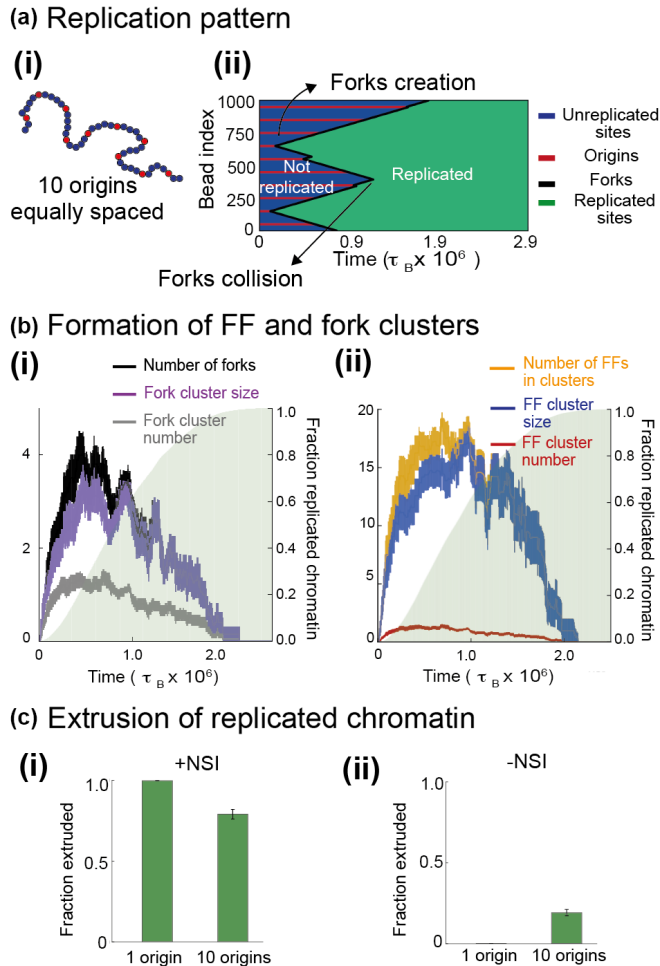


FIG. 5. Replication of a chromatin fiber with 10 equally spaced origins. (a) Sketch of the chromatin polymer containing multiple origins [panel (i)] and an example of a kymograph [panel (ii)]. The y-axis provides the chromatin bead number, and the x-axis the simulation time. Blue, red, black, and green pixels indicate the bead type (unreplicated sites, origins, forks, and replicated sites, respectively). Fork creations and collisions appear as green peaks and valleys. (b) Time evolution of the average size and number of clusters of forks [panel (i)] and of FFs [panel (ii)]. The number of forks and FFs within clusters and the fraction of replicated chromatin are also shown (the latter is represented by the green area and refers to the right y-axis). A cluster comprises particles (forks or FFs) whose 3D distance is smaller than 4σ for forks and 2σ for FFs. Averages are from 20 independent simulations. (c) Panel (i): fraction of extruded beads in simulations including nonspecific FF-chromatin interactions (+NSI) in the 1-origin setup (as in Fig. 3) and in the 10-origin setup (as in the two panels above). In the 10-origin case, the competition between origins and pairs of forks slightly decreases the likelihood of the immobile replisome scenario (which nevertheless remains dominant). Panel (ii): fraction of extruded beads in simulations without nonspecific FF-chromatin interactions (–NSI) in the 1-origin and 10-origin setup. In this case, the fraction of extruded beads is larger in the 10-origin setup. Plots were obtained by averaging over 10 (1-origin case without nonspecific interactions) or 20 (the other three cases) independent simulations.

kinetics is given by analyzing the time behavior of the FF clusters. Figure 5(b) (ii) shows that, after a small increment,

the number of FF clusters starts decreasing, while their size and the number of FFs in clusters increase for a while before decreasing again toward the end of replication. Interestingly, the number of FFs in clusters reaches its maximum slightly earlier than the curve referring to the average cluster size ($0.8 \times 10^6 \tau_B$ and $1.1 \times 10^6 \tau_B$, respectively). At this stage, the number of FFs in clusters is stable, while the average cluster size increases and the average number of clusters decreases; this weak anticorrelation indicates coarsening of actively replicating clusters, in broad qualitative agreement with the dynamics of replication factories seen by microscopy [51]. More striking results are obtained when the number of FFs is increased (see Fig. S5): in these cases, the average number of fork and FF clusters is larger, and the coarsening effects, due to the combination of BIPS with the motor activity of FFs, and indicated by a weak anticorrelation between FF cluster size and FF cluster number at intermediate times, are more visible.

F. The balance between extrusion and tracking depends on the number of origins

We now ask whether and how often, in a multiorigin setup, replicated chromatin is extruded by pairs of forks close in 3D, and if extrusion is observed also in the case in which nonspecific interactions between FFs and unreplicated chromatin are removed. As in Fig. 4, we quantify extrusion by computing the fraction of extruded beads. Different scenarios are analyzed in Fig. 5(c). First, with nonspecific FF-chromatin interactions (+NSI), extrusion is dominant both in the 1-origin and 10-origin setups [see Fig. 5(c) (i)]. However, in the presence of multiple origins, the overall fraction of extruded beads is slightly smaller, indicating that the competition for a finite amount of FFs among several origins and forks slightly destabilizes replication factories in favor of tracking replisomes (see Fig. S6). Second, if nonspecific interactions between FFs and chromatin are removed [–NSI, Fig. 5(c) (ii)], no beads are extruded in the 1-origin case (as seen in the phase diagram in Fig. 4), while 20% of beads are still extruded in the 10-origin setup. This is because, without nonspecific interactions, the presence of multiple origins and forks favors the formation of clusters of forks, or replication factories, which replicate some neighboring chromatin beads through extrusion.

Therefore, our results show that the presence of multiple origins affects the balance between extrusion (from replication factories) and tracking. Additionally, nonspecific interactions and multiple origins improve the efficiency of replication overall by reducing the replication time (see Fig. S7).

An interesting point emerges by looking at the effects of the 1D arrangement of the origins along the chromatin filament, which are uniformly spaced in Fig. 5. If the average distance between two consecutive origins is kept fixed, the average fraction of extruded beads is almost identical, whether the origins are equally spaced or randomly distributed (see Fig. S8-c). Still, origin distribution has subtle effects, as the proximity between origins locally favors extrusion (Fig. S8-d-e).

G. Mechanisms driving cluster growth

Above we observed that fork and FF clusters tend to become larger during replication. While this phenomenon is

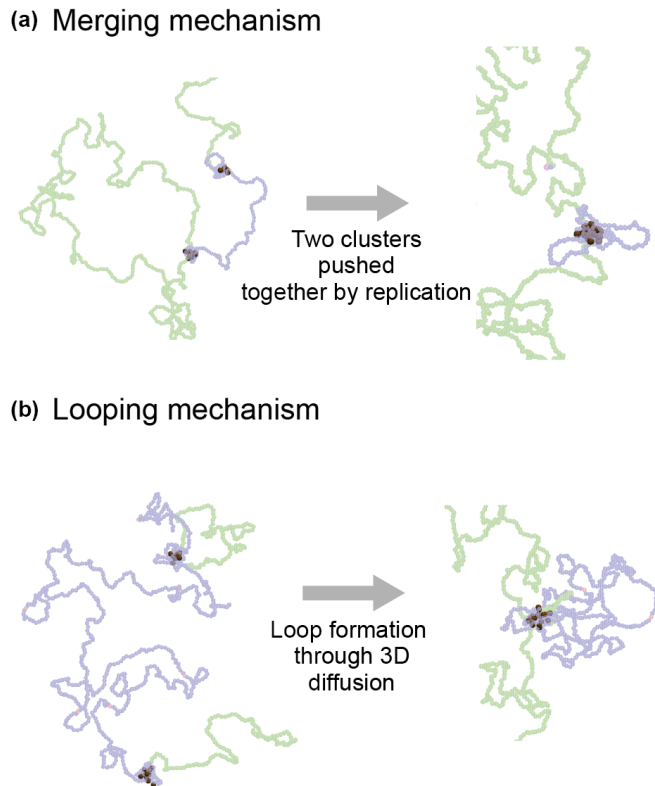


FIG. 6. Snapshots illustrating two mechanisms leading to the growth of FF clusters. (a) Merging mechanism: two FF clusters, pushed by the replication process, travel along the chromatin fiber getting closer to each other (left panel). Eventually, they meet and merge, forming a bigger cluster and a few short-range chromatin loops (right panel); the two small blue loops give an example of such loops). Beads composing the chromatin fiber are transparent to highlight FF clusters. (b) Looping mechanism: two FF clusters are far apart along the contour length of the chromatin fiber (left panel), but Langevin dynamics bring them close in 3D resulting in their merging and in the formation of long-ranged loops (right panel).

experimentally observed too, the mechanisms behind it are not fully understood [11]. We therefore now use PolyRep to investigate how clusters grow, focusing in particular on FF clusters. In the 10-origin system, two mechanisms for the growth of FF clusters can be identified, and they are illustrated using snapshots from two different simulations. The first, a *merging mechanism*, is shown in Fig. 6(a). Here, two FF clusters track along the template chromatin fiber pushed by the replication process [Fig. 6(a), left panel]: when they are close along the fiber, they merge forming short-range chromatin loops [Fig. 6(a), right panel]. The second, an unexpected *looping mechanism* [Fig. 6(b)], involves two clusters, far along the chromatin fiber, which get closer in 3D through diffusion and merge to form a single bigger cluster. Here, coarsening is associated with the formation of long-ranged chromatin loops. Importantly, while the merging mechanism is led by the action of molecular motors involved in replication, the looping mechanism is due to the 3D diffusion of the chromatin filament and firing factors.

Combined, these mechanisms mimic the enlargement of foci and their movement along the genome seen *in vivo*

[10,49]. While the merging mechanism has been described previously [13], the looping mechanism has not been discussed yet, and we suggest it would be interesting to look for it in future experiments. Our simulations also suggest that FF clusters can increase in size by following an *unbinding-rebinding mechanism* where some FFs, belonging to a cluster, abandon the chromatin fiber to bind it again in the proximity of another cluster (Fig. S9). Note, however, that this phenomenon does not increase the size of the underlying fork cluster.

III. DISCUSSION

In summary, we have presented PolyRep, a 3D model for chromatin replication, and characterized its emergent behavior. This model fundamentally differs from most previous DNA replication models, which are effectively one-dimensional [23,52,53]. Unlike previous 3D models for DNA replication [25], ours focuses on chromatin rather than bacteria and explicitly includes active firing factors—which model generic complexes of replisome components, such as DNA polymerases and helicases. This allows us to study the effect of different types of chromatin-protein interactions, such as the balance between nonspecific attraction between FFs and unreplicated chromatin, and the specific attraction to origins and forks. We also model replication dynamics and ask questions on the time evolution of 3D chromatin and protein structures at mobile forks. Besides recapitulating known features of chromatin replication, our model allows us to make mechanistic predictions that are experimentally testable. After this work was finished, a related work appeared, which employs a lattice model to investigate the role of fork interactions on the 3D genome structure of replicating chromatin [54]. With respect to our work, Ref. [54] does not include explicit firing factors, and it focuses on chromatin interactions and comparison with Hi-C. Instead, here we focus on the spatiotemporal patterns and dynamics of clusters of forks and firing factors in 3D.

Our main result is that such clusters spontaneously form during replication: they diffuse slowly while extruding loops of replicated chromatin. The extrusion of replicating chromatin loops is qualitatively consistent with the biological models of immobile replisomes [6] and of replication factories [2]; another related biophysical model is that of loop extrusion via SMC proteins, although in our case clustering of FFs and forks is required to extrude replication loops so that extrusion is an emergent property of the model. More specifically, we predict that extrusion requires two main ingredients: (i) a motor activity of FFs at replication forks, which is natural to assume as they model complexes of molecular motors such as DNA polymerases and helicases, and (ii) cluster formation. The latter occurs through an active generalization of bridging-induced phase separation (BIPS) [43,55], which stands for the generic tendency of multivalent proteins interacting with chromatin to cluster.

BIPS in our context necessitates nonspecific interactions to occur, and indeed when abrogating them both BIPS and extrusion are not observed in the simulations—instead replisomes separately track on chromatin. Nonspecific interactions, already observed for some eukaryotic transcription factors [56],

are likely important *in vivo* and BIPS may underlie the formation of clusters of pre-replication complexes [57]. Before replication, BIPS creates microphase-separated aggregates [58] due to the combination of nonspecific attraction to non-replicated chromatin and specific interactions to the origins. These aggregates later nucleate sites where replication initiates mimicking what happens *in vivo*, where transcriptional hubs colocalize with early replication factories [59].

Our dynamic model can be used to study the morphology and dynamics of clusters of FFs and forks. Regarding morphology, we observe that clusters typically involve a significantly larger number of factors with respect to forks. Concerning the dynamics, we observe a nonmonotonic behavior, where clusters first grow and then shrink as replication terminates. This is qualitatively similar to what was observed in cells [51].

Inspection of the dynamical trajectories of our model allows us to identify all the kinetic events through which replication clusters may grow or evolve in S-phase. First, forks or replisomes may collide and merge. Second, we find a distinct mechanism through which replication factories that are far apart along the chromatin colocalize in space via the formation of a long-range chromatin loop. We speculate that this fully 3D mechanism would ignite the firing of an origin by forming a chromatin loop between the inactive origin and a replication cluster. It would be interesting to seek evidence of this looping-mediated origin activation in the future, possibly by analyzing correlations between data on origin activities over time and Hi-C maps of chromosome contacts in the S-phase.

Our model also gives interesting insights into potential mechanisms both to explain the fast DNA polymerase unbinding-rebinding dynamics recently observed through single fluorescent proteins experiments [60], and to avoid the formation of stalled forks or to continue replication in case one fork is stopped by the presence of a chromosome lesion (see Fig. S10). Even if our model does not include transcription-related molecules or DNA breaks, it still predicts the formation of temporarily inactive forks where thermal noise leads to factor disengagement from a fork. The corresponding continuous binding and unbinding of FFs predicted by our model is in line with the process of replication of Okazaki fragments [61], and also with recent experiments where components of yeast replisomes are observed only to be transiently bound to replication forks [17]. In our simulations, these temporarily inactive structures can be readily rescued, as the weak attraction between unreplicated chromatin and FFs facilitates the reassembly of an FF cluster close to them. This may avoid the formation of permanently stalled forks, which would instead biologically require the DNA damage response to be reactivated.

More generally, nonspecific attraction might act not only between forks and FFs, but also between forks and biomolecules that are known to be involved in repairing stalled forks such as the enzyme RecG, which is needed to restart replication of temporarily inactive forks in the *E. Coli* genome [62]. In the future, it would be interesting to experimentally investigate whether the reactivation of such forks is easier when these are embedded in unreplicated euchromatin, due to nonspecific interactions, as predicted by our model.

Finally, in light of recent observations correlating replication origins' efficiency and position to TAD boundaries [63,64], in future research it may be of interest to include in the model an active cohesin loop extrusion, and to see how this couples to the emergent replication-driven (or polymerase-driven) extrusion activity we found here.

IV. MATERIALS AND METHODS

Molecular-dynamics simulations

Chromatin is modeled as a semiflexible polymer of N beads, each with diameter $\sigma = 15$ nm (corresponding to 1 kbp). Bonds between consecutive beads are treated as harmonic springs,

$$V_H(r) = K_H(r - R_H)^2, \quad (4)$$

with typical spring length $R_H = 1.1\sigma$ and spring constant $K_{HA} = 200k_B T/\sigma^2$, where k_B is the Boltzmann constant, and $T = 300$ K the temperature of the system. The polymer stiffness is modeled by a Kratky-Porod potential:

$$V_B(\phi) = K_B(1 + \cos \phi), \quad (5)$$

with ϕ being the angle between three consecutive beads, and K_B is the rigidity coefficient. The latter is set equal to $K_B = 4k_B T$ to give a persistence length $l_p \sim 60$ nm (compatible to that of chromatin [34]). The excluded-volume interaction between nonconsecutive beads at spatial distance r is modeled by the Weeks-Chandler-Anderson (WCA) potential

$$V_{WCA}(r) = 4k_B T \left[\left(\frac{\sigma}{r} \right)^{12} - \left(\frac{\sigma}{r} \right)^6 + \frac{1}{4} \right] \Theta(2^{1/6}\sigma - r). \quad (6)$$

The polymer is in dilute conditions, immersed in a cubic simulation box of size 110σ with freely diffusing brown FFs. The initial configuration involves unreplicated chromatin sites and origins [blue and red beads in Fig. 2(a)]. After a pre-equilibration for a time $T_{eq,pol} = 1.5 \times 10^6 \tau_{LJ}$ (where τ_{LJ} is the Lennard-Jones time unit for simulations), FFs (brown spheres in Fig. 2) are initially inserted in random positions into the volume. Then, a soft potential V_{SOFT} is applied between them and beads in the polymer for a time $T_{SOFT} = 10^3 \tau_{LJ}$ to displace those FFs that overlap beads in the chain. The soft potential is described by

$$V_{SOFT}(r) = A \left[1 + \cos \left(\frac{\pi r}{r_c} \right) \right] \Theta(r - r_c), \quad (7)$$

where $A = 100k_B T$ describes the strength of the potential, and $r_c = 2^{1/6}\sigma$ is the threshold below which the potential is effective. Consequently, the system is further equilibrated by inserting only steric repulsions between FFs and beads in the chain for an additional time $T_{steric} = 10^3 \tau_{LJ}$. Replication initiates [Fig. 2(b)] after a time $T_{eq,tot} = T_{eq,pol} + T_{SOFT} + T_{steric}$ by switching on an attractive interaction between FFs and the chain that is described by a truncated and shifted Lennard-Jones potential:

$$V_{LJ/cut}(r) = [V_{LJ}(r) - V_{LJ}(r_c)] \Theta(r_c - r), \quad (8)$$

with

$$V_{LJ}(r) = 4\epsilon \left[\left(\frac{\sigma}{r} \right)^{12} - \left(\frac{\sigma}{r} \right)^6 \right]. \quad (9)$$

We consider a cutoff distance $r_c = 1.8\sigma$, while the attraction strength is $\varepsilon_{\text{origin}} = 6k_B T$ between FFs and origins, and $\varepsilon_{\text{ns}} = 4k_B T$ between FFs and unreplicated chromatin beads (except in cases in which the last two parameters are changed to investigate extrusion of replicated chromatin, for example in Fig. 4). If an origin at site i has at least one FF at a distance $r < r_c = 1.8\sigma$, it fires with probability P_{fire} to create a pair of forks (black beads in Fig. 2) that experience an attraction $\varepsilon_{\text{fork}} = 10k_B T$ with FFs. If beads $i - 1$ and $i + 1$ are unreplicated chromatin sites or replication origins, the pair of forks are created in $(i - 1, i)$ or $(i, i + 1)$ with equal probability. If $i + 1$ (or $i - 1$) is occupied by another preexisting fork, the pair of forks is created at $(i - 1, i)$ [or at $(i, i + 1)$]. If $i = 1$, the forks are created at $(1, 2)$; if $i = N$, the forks will be placed at $(N - 1, N)$. Finally, if neither site $i + 1$ nor $i - 1$ is available, the pair of forks is not created. Once created, the two forks move stepwise along the polymer independently and in opposite directions whenever a FF is located at a distance $d \leq 1.8\sigma$ from them [Fig. 2(c)]. Supposing that a fork is in position i and that an FF is close by, a replication step involves the fork moving, for instance, to the site $i + 1$, while the site i becomes replicated chromatin and a newly synthesized chromatin bead is inserted in the system (green beads in Fig. 2). Both replicated fibers are connected to the forks they originated from through harmonic potentials as in Eq. (4) and they both also provide the same energy contribution: a Kratky-Porod potential [Eq. (5)] to represent the polymer's stiffness, a harmonic interaction [Eq. (4)] for bonded beads belonging to one of the two polymers, and a repulsive soft potential [Eq. (7)] to describe the interaction between green synthesized beads and any other nonbonded bead (FFs, chromatin beads from the same replicated fiber and chromatin beads from other replicated or unreplicated fibers). When two forks collide, they disappear to leave two joined fibers of green replicated beads that cannot be re-replicated as they contain no replication origin and have no affinity for brown beads [Fig. 2(d)]. Once a fork reaches an extremity of the template polymer and replicates it, the two newly replicated fibers are no longer joined together and diffuse independently.

The dynamics of a bead at position \mathbf{r}_i is described by the Langevin equation:

$$m_i \frac{\partial^2 \mathbf{r}_i}{\partial t^2} = \nabla_i U - \gamma_i \frac{\partial \mathbf{r}_i}{\partial t} + \sqrt{2k_B T \gamma_i} \eta_i, \quad (10)$$

where U is the total energy of the system, and γ_i is the friction on the i th bead due to the solvent. The term η_i represents

thermal noise whose components are such that

$$\langle \eta_{i\alpha}(t) \rangle = 0 \quad \text{and} \quad \langle \eta_{i\alpha}(t) \eta_{j\beta}(t') \rangle = \delta_{ij} \delta_{\alpha\beta} \delta(t - t'),$$

where δ_{ij} and $\delta_{\alpha\beta}$ are the Kronecker delta and $\delta(t - t')$ is the Dirac delta. Simulations are performed using the software LAMMPS for molecular dynamics [42] (using a time step $dt = 0.01\tau_{\text{LJ}}$) and an external C++ code called by the LAMMPS script. The C++ code is needed to implement fork movements and synthesize the newly replicated fiber. The simulation time between two consecutive calls of code by a LAMMPS script, T_{call} , is related to the fork velocity through the relationship $v_{\text{fork}} = \frac{1}{T_{\text{call}}} \sigma / \tau_{\text{LJ}}$ as a fork moves 1σ between two consecutive calls of the code (in the presence of at least one nearby FF). We first map the simulation time to real times to express the fork velocity in real units. Three typical times are important to describe the system: the Brownian time $\tau_B = \sigma^2 / D_B$ (where D_B is the diffusion coefficient), the autocorrelation time $\tau_{\text{dec}} = m / \gamma$ (where γ is the friction of the solvent), and the Lennard-Jones time $\tau_{\text{LJ}} = \sigma \sqrt{m / k_B T}$. We can observe that $\tau_{\text{LJ}} = \tau_{\text{dec}} = \tau_B$, as in simulation units $\sigma = \gamma = k_B T = m = 1$ and $D_B = k_B T / \gamma$. One can then use τ_B to map time from simulation to real units. By employing the Stokes-Einstein equation for spherical beads, $\gamma = 3\pi\sigma\eta_{\text{sol}}$, we obtain $\tau_B = \frac{3\pi\sigma^3\eta_{\text{sol}}}{k_B T}$, which, for $\sigma = 1 \text{ kbp} \sim 15 \text{ nm}$, $T = 300 \text{ K}$, and $\eta_{\text{sol}} \sim 150 \text{ cP}$, provides $\tau_B \sim 1 \text{ ms}$. In our simulations, we use $T_{\text{call}} = (3 \times 10^3 \tau_B) - (5 \times 10^3 \tau_B)$ resulting in $v_{\text{fork}} \sim 12\text{--}20 \text{ kbp/min}$, which is relatively close to the average fork velocity in eukaryotes [14].

In the 1-origin case, the chain contains 1000 beads (representing 1 Mbp), with a single replication origin in the middle (at bead 501; beads are numbered 1 to 1000). In the 10-origin case, the chain contains 1000 beads with 10 equally spaced origins (at beads 50, 150, 250, ..., 950, so origins are 100 kbp apart).

ACKNOWLEDGMENTS

We thank C. A. Brackley and D. Jost for useful discussions. This work was supported by the Wellcome Trust (223097/Z/21/Z). E.O. acknowledges support from Grant No. PRIN 2022R8YXMR funded by the Italian Ministry of University and Research.

G.F. performed simulations. G.F., D.M., and E.O. analyzed the data and designed the research. All authors contributed to writing the manuscript.

The authors declare no competing interests.

-
- [1] B. Alberts, A. Johnson, J. Lewis, D. Morgan, K. Roberts, and P. Walter, *Molecular Biology of the Cell*, Sixth Edition (Garland Science, New York, 2014).
- [2] P. R. Cook, The organization of replication and transcription, *Science* **284**, 1790 (1999).
- [3] D. Bates, The bacterial replisome: Back on track? *Mol. Microbiol.* **69**, 1341 (2008).
- [4] J. T. Yeeles, T. D. Deegan, A. Janska, A. Early, and J. F. Diffley, Regulated eukaryotic DNA replication origin firing with purified proteins, *Nature (London)* **519**, 431 (2015).
- [5] H. Yardimci, A. B. Loveland, S. Habuchi, A. M. Van Oijen, and J. C. Walter, Uncoupling of sister replisomes during eukaryotic DNA replication, *Mol. Cell* **40**, 834 (2010).
- [6] Z. Yuan, R. Georgescu, R. de L. A. Santos, D. Zhang, L. Bai, N. Y. Yao, G. Zhao, M. E. O'Donnell, and H. Li, Ctf4 organizes sister replisomes and Pol α into a replication factory, *eLife* **8**, e47405 (2019).
- [7] H. Li, N. Y. Yao, and M. E. O'Donnell, Anatomy of a twin DNA replication factory, *Biochem. Soc. Trans.* **48**, 2769 (2020).

- [8] P. J. Chen, A. B. McMullin, B. J. Visser, Q. Mei, S. M. Rosenberg, and D. Bates, Interdependent progression of bidirectional sister replisomes in *E. coli*, *eLife* **12**, e82241 (2023).
- [9] W. Xiang, M. J. Roberti, J.-K. Hériché, S. Huet, S. Alexander, and J. Ellenberg, Correlative live and super-resolution imaging reveals the dynamic structure of replication domains, *J. Cell Biol.* **217**, 1973 (2018).
- [10] A. E. Vouzas and D. M. Gilbert, Mammalian DNA replication timing, *Cold Spring Harb. Perspect. Biol.* **13**, a040162 (2021).
- [11] V. O. Chagin, C. S. Casas-Delucchi, M. Reinhart, L. Schermelleh, Y. Markaki, A. Maiser, J. J. Bolius, A. Bensimon, M. Fillies, P. Domaing, Y. M. Rozanov, H. Leonhardt, and M. C. Cardoso, 4D visualization of replication foci in mammalian cells corresponding to individual replicons, *Nat. Commun.* **7**, 11231 (2016).
- [12] B. Anachkova, V. Djeliova, and G. Russev, Nuclear matrix support of DNA replication, *J. Cell. Biochem.* **96**, 951 (2005).
- [13] P. Meister, A. Taddei, A. Ponti, G. Baldacci, and S. M. Gasser, Replication foci dynamics: Replication patterns are modulated by S-phase checkpoint kinases in fission yeast, *EMBO J.* **26**, 1315 (2007).
- [14] A. Gispán, M. Carmi, and N. Barkai, Model-based analysis of DNA replication profiles: Predicting replication fork velocity and initiation rate by profiling free-cycling cells, *Genome Res.* **27**, 310 (2017).
- [15] M. Berti and A. Vindigni, Replication stress: Getting back on track, *Nat. Struct. Mol. Biol.* **23**, 103 (2016).
- [16] A. Franchitto, Genome instability at common fragile sites: Searching for the cause of their instability, *Biomed Res. Int.* **2013**, 730714 (2013).
- [17] T. R. Beattie, N. Kapadia, E. Nicolas, S. Uphoff, A. J. Wollman, M. C. Leake, and R. Reyes-Lamothe, Frequent exchange of the DNA polymerase during bacterial chromosome replication, *eLife* **6**, e21763 (2017).
- [18] S. H. Mueller, L. M. Spenkelink, and A. M. van Oijen, When proteins play tag: The dynamic nature of the replisome, *Biophys. Rev.* **11**, 641 (2019).
- [19] A. Shaw, P. Olivares-Chauvet, A. Maya-Mendoza, and D. A. Jackson, S-phase progression in mammalian cells: Modelling the influence of nuclear organization, *Chromos. Res.* **18**, 163 (2010).
- [20] R. Retkute, C. A. Nieduszynski, and A. de Moura, Mathematical modeling of genome replication, *Phys. Rev. E* **86**, 031916 (2012).
- [21] Y. Gindin, M. S. Valenzuela, M. I. Aladjem, P. S. Meltzer, and S. Bilke, A chromatin structure-based model accurately predicts DNA replication timing in human cells, *Mol. Syst. Biol.* **10**, 722 (2014).
- [22] S. P. Das, T. Borrmann, V. W. T. Liu, S. C.-H. Yang, J. Bechhoefer, and N. Rhind, Replication timing is regulated by the number of MCMs loaded at origins, *Genome Res.* **25**, 1886 (2015).
- [23] D. Löb, N. Lengert, V. O. Chagin, M. Reinhart, C. S. Casas-Delucchi, M. C. Cardoso, and B. Drossel, 3D replicon distributions arise from stochastic initiation and domino-like DNA replication progression, *Nat. Commun.* **7**, 11207 (2016).
- [24] J.-M. Arbona, A. Goldar, O. Hyrien, A. Arneodo, and B. Audit, The eukaryotic bell-shaped temporal rate of DNA replication origin firing emanates from a balance between origin activation and passivation, *eLife* **7**, e35192 (2018).
- [25] S. Jun and B. Mulder, Entropy-driven spatial organization of highly confined polymers: Lessons for the bacterial chromosome, *Proc. Natl. Acad. Sci. USA* **103**, 12388 (2006).
- [26] S. Bianco, A. M. Chiariello, M. Conte, A. Esposito, L. Fiorillo, F. Musella, and M. Nicodemi, Computational approaches from polymer physics to investigate chromatin folding, *Curr. Opin. Cell Biol.* **64**, 10 (2020).
- [27] R. Natesan, K. Gowrishankar, L. Kuttippurathu, P. S. Kumar, and M. Rao, Active remodeling of chromatin and implications for in vivo folding, *J. Phys. Chem. B* **126**, 100 (2022).
- [28] S. Kadam, K. Kumari, V. Manivannan, S. Dutta, M. K. Mitra, and R. Padinhateeri, Predicting scale-dependent chromatin polymer properties from systematic coarse-graining, *Nat. Commun.* **14**, 4108 (2023).
- [29] Y. Hu and B. Stillman, Origins of DNA replication in eukaryotes, *Mol. Cell* **83**, 352 (2023).
- [30] W. Wang, K. N. Klein, K. Proesmans, H. Yang, C. Marchal, X. Zhu, T. Borrmann, A. Hastie, Z. Weng, J. Bechhoefer *et al.*, Genome-wide mapping of human DNA replication by optical replication mapping supports a stochastic model of eukaryotic replication, *Mol. Cell* **81**, 2975 (2021).
- [31] P. A. Zhao, T. Sasaki, and D. M. Gilbert, High-resolution Repli-Seq defines the temporal choreography of initiation, elongation and termination of replication in mammalian cells, *Genome Biol.* **21**, 76 (2020).
- [32] N. Rhind, DNA replication timing: Biochemical mechanisms and biological significance, *BioEssays* **44**, 2200097 (2022).
- [33] M. Chiang, G. Forte, N. Gilbert, D. Marenduzzo, and C. A. Brackley, Predictive polymer models for 3D chromosome organization, *Meth. Mol. Biol.* **2301**, 267 (2022).
- [34] J. Langowski, Polymer chain models of DNA and chromatin, *Eur. Phys. J. E* **19**, 241 (2006).
- [35] J. Langowski and D. W. Heermann, Computational modeling of the chromatin fiber, in *Seminars in Cell & Developmental Biology* (Elsevier, Amsterdam, 2007), Vol. 18, pp. 659–667.
- [36] M. Fragkos, O. Ganier, P. Coulombe, and M. Méchali, DNA replication origin activation in space and time, *Nat. Rev. Mol. Cell Biol.* **16**, 360 (2015).
- [37] M. Stracy, J. Schweizer, D. J. Sherratt, A. N. Kapanidis, S. Uphoff, and C. Lesterlin, Transient non-specific DNA binding dominates the target search of bacterial DNA-binding proteins, *Mol. Cell* **81**, 1499 (2021).
- [38] M. Sheinman, O. Bénichou, Y. Kafri, and R. Voituriez, Classes of fast and specific search mechanisms for proteins on DNA, *Rep. Prog. Phys.* **75**, 026601 (2012).
- [39] P. R. Cook, *Principles of Nuclear Structure and Function* (John Wiley & Sons, Hoboken, NJ, 2001).
- [40] Z. Jasencakova and A. Groth, Restoring chromatin after replication: How new and old histone marks come together, in *Seminars in Cell & Developmental Biology* (Elsevier, Amsterdam, 2010), Vol. 21, pp. 231–237.
- [41] C. Alabert and A. Groth, Chromatin replication and epigenome maintenance, *Nat. Rev. Mol. Cell Biol.* **13**, 153 (2012).
- [42] S. Plimpton, Fast parallel algorithms for short-range molecular dynamics, *J. Comput. Phys.* **117**, 1 (1995).
- [43] C. A. Brackley, S. Taylor, A. Papanonis, P. R. Cook, and D. Marenduzzo, Nonspecific bridging-induced attraction drives clustering of DNA-binding proteins and genome organization, *Proc. Natl. Acad. Sci. USA* **110**, E3605 (2013).

- [44] C. Brackley, Polymer compaction and bridging-induced clustering of protein-inspired patchy particles, *J. Phys.: Condens. Matter* **32**, 314002 (2020).
- [45] See Supplemental Material at <http://link.aps.org/supplemental/10.1103/PRXLife.2.033014> for additional text, figures, and movies.
- [46] J. M. Berg, J. L. Tymoczko, and L. Stryer, *Biochemistry (Loose-Leaf)* (W. H. Freeman, New York, 2007).
- [47] M. Hawkins, R. Retkute, C. A. Müller, N. Saner, T. U. Tanaka, A. P. de Moura, and C. A. Nieduszynski, High-resolution replication profiles define the stochastic nature of genome replication initiation and termination, *Cell Rep.* **5**, 1132 (2013).
- [48] H. Leonhardt, H.-P. Rahn, P. Weinzierl, A. Sporbert, T. Cremer, D. Zink, and M. C. Cardoso, Dynamics of DNA replication factories in living cells, *J. Cell. Biol.* **149**, 271 (2000).
- [49] H. Nakamura, T. Morita, and C. Sato, Structural organizations of replicon domains during DNA synthetic phase in the mammalian nucleus, *Exp. Cell Res.* **165**, 291 (1986).
- [50] S. D. Stoddard, Identifying clusters in computer experiments on systems of particles, *J. Comput. Phys.* **27**, 291 (1978).
- [51] P. Hozák, D. A. Jackson, and P. R. Cook, Replication factories and nuclear bodies: The ultrastructural characterization of replication sites during the cell cycle, *J. Cell Sci.* **107**, 2191 (1994).
- [52] A. P. de Moura, R. Retkute, M. Hawkins, and C. A. Nieduszynski, Mathematical modelling of whole chromosome replication, *Nucl. Acids Res.* **38**, 5623 (2010).
- [53] T. Kelly and A. J. Callegari, Dynamics of DNA replication in a eukaryotic cell, *Proc. Natl. Acad. Sci. USA* **116**, 4973 (2019).
- [54] D. D'Asaro, M. M. C. Tortora, C. Vaillant, J.-M. Arbona, and D. Jost, DNA replication and polymer chain duplication reshape the genome in space and time, *bioRxiv* 2024.03.12.584628 (2024).
- [55] J.-K. Ryu, C. Bouchoux, H. W. Liu, E. Kim, M. Minamino, R. de Groot, A. J. Katan, A. Bonato, D. Marenduzzo, D. Michieletto *et al.*, Bridging-induced phase separation induced by cohesin SMC protein complexes, *Sci. Adv.* **7**, eabe5905 (2021).
- [56] M. Mazzocca, T. Fillot, A. Loffreda, D. Gnani, and D. Mazza, The needle and the haystack: Single molecule tracking to probe the transcription factor search in eukaryotes, *Biochem. Soc. Trans.* **49**, 1121 (2021).
- [57] J. Li, J. Dong, W. Wang, D. Yu, X. Fan, Y. C. Hui, C. S. Lee, W. H. Lam, N. Alary, Y. Yang *et al.*, The human pre-replication complex is an open complex, *Cell* **186**, 98 (2023).
- [58] C. A. Brackley, J. Johnson, S. Kelly, P. R. Cook, and D. Marenduzzo, Simulated binding of transcription factors to active and inactive regions folds human chromosomes into loops, rosettes and topological domains, *Nucl. Acids Res.* **44**, 3503 (2016).
- [59] A. B. Hassan, R. J. Errington, N. S. White, D. A. Jackson, and P. R. Cook, Replication and transcription sites are colocalized in human cells, *J. Cell Sci.* **107**, 425 (1994).
- [60] L. Xu, M. T. J. Halma, and G. J. L. Wuite, Mapping fast DNA polymerase exchange during replication, *Nat. Commun.* **15**, 5328 (2024).
- [61] T. Ogawa and T. Okazaki, Discontinuous DNA replication, *Annu. Rev. Biochem.* **49**, 421 (1980).
- [62] P. R. Bianco and Y. Lu, Single-molecule insight into stalled replication fork rescue in *Escherichia coli*, *Nucl. Acids Res.* **49**, 4220 (2021).
- [63] D. J. Emerson, P. A. Zhao, A. L. Cook, R. J. Barnett, K. N. Klein, D. Saulebekova, C. Ge, L. Zhou, Z. Simandi, M. K. Minsk *et al.*, Cohesin-mediated loop anchors confine the locations of human replication origins, *Nature (London)* **606**, 812 (2022).
- [64] Y. Li, B. Xue, M. Zhang, L. Zhang, Y. Hou, Y. Qin, H. Long, Q. P. Su, Y. Wang, X. Guan *et al.*, Transcription-coupled structural dynamics of topologically associating domains regulate replication origin efficiency, *Genome Biol.* **22**, 206 (2021).